Comparative proteomics reveals signature metabolisms of exponentially growing and stationary phase marine bacteria

Exponentially growing bacteria are rarely found in nature. Instead, bacteria spend most of their lifetime in a slow- or non-proliferating state, a state that is occasionally interrupted by an increase in accessible nutrients. To successfully compete for pulses of nutrients, copiotrophic marine bacteria have adaptations that allow them to change their metabolism to support exponential growth in response to nutrients and to return to stationary phase when nutrients return to normal scarcity. The molecular details of these adaptations can be observed through proteome profiles, i.e. relative abundances of proteins in cells, and how they change between different conditions. We developed proteome profiles during exponential and stationary phase conditions for three model organisms representing major marine bacterioplankton lineages. 22500-3000 proteins per isolate were detected, representing large proportions of each proteome (67-87%). A shift from protein synthesis and other processes typically associated with active growth, to proteins essential for nutrient scavenging, was observed during transition into stationary phase. The three isolates differed in magnitude of their responses and in how enzymes of different metabolisms responded. Some of the differences can be seen as differences in implementation of a shared strategy, such as an increase in enzymes involved in carbon storage, while other differences are best described as differences in strategy. We thus observed the proteome reflection of "signature metabolisms" in the three isolates – distinct metabolic adaptations to environmental circumstances. These findings have direct implications for the interpretation of proteomic and genetic data from microbes in natural environments.

Comparative proteomics reveals signature metabolisms of exponentially growing and stationary phase marine bacteria

Saraladevi Muthusamy[1], Daniel Lundin[1*], Rui Miguel Mamede Branca[2], Federico Baltar[1,3], José M. González[4], Janne Lehtiö[2] and Jarone Pinhassi[1]

[1]Centre for Ecology and Evolution in Microbial model Systems - EEMiS, Linnaeus University, SE-39182 Kalmar, Sweden.

[2]Clinical Proteomics Mass Spectrometry, Department of Oncology-Pathology, Science for Life Laboratory and Karolinska Institute, Stockholm, Sweden.

[3]Department of Marine Science, University of Otago, Dunedin, New Zealand.

[4]Department of Microbiology, University of La Laguna, ES-38206 La Laguna, Tenerife, Spain.

[*]Corresponding author: Daniel Lundin, Centre for Ecology and Evolution in Microbial model Systems - EEMiS, Barlastgatan 11, Linnaeus University, SE-39182 Kalmar, Sweden. e-mail: daniel.lundin@lnu.se

Running title: Proteomics of marine copiotrophs

Keywords: Microbiology, proteomics, marine bacteria, signature metabolism, copiotrophs, heterotrophs, exponential growth, stationary phase, growth phase

1

IMPORTANCE

Much of the phenotype of microorganisms consists of its repertoire of metabolisms and the dynamics of their expression. The metabolic dynamics of an organism is in turn manifested through regulated expression of proteins, mostly enzymes and transporters. When an organism changes its activity focus, the change is thus performed through changes in synthesis of proteins. It is hence of importance to microbial ecologists to characterize the protein content of microorganisms under different growth conditions and to profile different species to gain a better understanding of how ecologically important nutrient scavenging strategies are implemented. Here, we analyze the protein profiles of representatives of three important marine bacterial lineages, and discover metabolic signatures in nutrient scavenging, energy and carbon metabolism specific for the species. Several of the differences can be seen as differences in implementation of a shared strategy, in the form of carbon source utilization and selection of storage compounds.

ABSTRACT

Exponentially growing bacteria are rarely found in nature. Instead, bacteria spend most of their lifetime in a slow- or non-proliferating state, a state that is occasionally interrupted by an increase in accessible nutrients. To successfully compete for pulses of nutrients, copiotrophic marine bacteria have adaptations that allow them to change their metabolism to support exponential growth in response to nutrients and to return to stationary phase when nutrients return to normal scarcity. The molecular details of these adaptations can be observed through proteome profiles, *i.e.* relative abundances of proteins in cells, and how they change between different conditions. We developed proteome profiles during exponential and stationary phase conditions for three model organisms representing major marine bacterioplankton lineages.

2500-3000 proteins per isolate were detected, representing large proportions of each proteome (67-87%). A shift from protein synthesis and other processes typically associated with active growth, to proteins essential for nutrient scavenging, was observed during transition into stationary phase. The three isolates differed in magnitude of their responses and in how enzymes of different metabolisms responded. Some of the differences can be seen as differences in implementation of a shared strategy, such as an increase in enzymes involved in carbon storage, while other differences are best described as differences in strategy. We thus observed the proteome reflection of "signature metabolisms" in the three isolates – distinct metabolic adaptations to environmental circumstances. These findings have direct implications for the interpretation of proteomic and genetic data from microbes in natural environments.

INTRODUCTION

Nutrient availability is a principal factor driving metabolic flux, growth and activity of microbes in natural seawater (1, 2). However, the distribution of nutrients is not uniform. Most of the ocean surface water column is depleted in nutrients such as nitrogen, phosphorus, iron and silicate (3-5), while *e.g.* coastal areas are heavily influenced by seasonal or episodic changes in nutrient concentration. The dynamics of nutrients in the environment induce certain classes of marine heterotrophic bacteria to shift between short periods of growth and active cell division during conditions of nutrient availability, and prolonged slow- or non-growth states under nutrient-limited conditions (6, 7). The trophic strategy characterized by shifts in metabolic regulation to capitalize on nutrient pulses is known as "copiotrophy" in contrast to "oligotrophy", characterized instead by lack of response (8). While largely beneficial in a fluctuating environment, growth phase transition comes at a cost, and involves a wide range of physiological adaptations (9, 10).

To understand the functioning of microbial communities in natural environments during fluctuations in nutrient concentrations, it is important to understand the individual responses of community members. Bacterial adaptation strategies during nutrient limitation have hence been studied comprehensively in model organisms like *Escherichia coli* and *Bacillus subtilis* (6, 11, 12). From these studies, it is clear that bacteria that enter into stationary phase undergo both morphological and physiological changes. As examples of changes of morphology, the Gammaproteobacteria *Vibrio cholerae* and *Pseudomonas fluorescens* decrease their cell size and undergo transition into a viable but non-culturable state as a response to low nutrients (13, 14). In *E. coli*, entry into stationary phase induces formation of spherical-shaped cells instead of rods and stimulates formation of aggregates (11), while *B. subtilis* cells produce spores in response to

4

starvation (12). The physiological response to transition from exponential growth to stationary phase often involves a shift from expression of proteins related to cell growth, cell division and protein biosynthesis (15, 16) to proteins needed to scavenge nutrients and to effectively compete with other populations (17). Moreover, proteins involved in stress responses, *e.g.* oxidative, heat and osmotic stress or nutrient stress like carbon and phosphate starvation, tend to be induced at the transition into stationary phase (18, 19). In *E. coli*, proteins related to energy metabolism, phosphotransferase and transport binding proteins are down regulated during stationary phase compared with exponential phase growth (20). In *B. subtilis*, proteins with functions in nutrient scavenging processes, proteases and extracellular enzymes become relatively more abundant during stationary phase (12). From work on model organisms we can thus conclude that responses to nutrient pulses differ between species, even among typical copiotrophs, which in turn suggests that a fuller understanding of natural communities could be gained by molecular analyses of isolates from marine environments.

Like model bacteria, marine bacteria in stationary phase undergo pronounced morphological changes; cells may aggregate or remain as single cells and also become smaller and spherical (7, 13, 21, 22). The planctomycete *Rhodopirellula baltica* produces alternative sigma factors and oxidative stress response proteins while protein biosynthesis is down-regulated during stationary phase (7). In Roseobacter clade members (Alphaproteobacteria), adjustments to stationary phase involve increased abundance of stress response proteins, membrane transporters and flagellar motility proteins, similar to how model organisms respond (23, 24). In contrast, the oligotrophic model bacterium *Candidatus* Pelagibacter ubique, a representative of the ubiquitous and abundant alphaproteobacterial SAR11 clade, lacks the global stationary phase sigma factor (σs) that is part of the stationary phase response in model organisms, and the majority of the

expressed proteins (92%) in this oligotroph remains unchanged during entry into the stationary

phase (21).

Barring the above-mentioned examples little is known about the variability in proteome

responses to onset of the famine phase of the feast and famine lifestyle typical of copiotrophs.

We sought to address this lack of understanding by investigating proteome profiles of three

different heterotrophic bacteria during transition from exponential growth to stationary phase.

Each bacterium represents major lineages of marine bacteria: *Neptuniibacter* sp. strain MED92

(Gammaproteobacteria, Oceanospirillaceae; MED92), *Phaeobacter* sp. strain MED193

(Alphaproteobacteria, member of the Roseobacter clade; MED193) and *Dokdonia* sp. strain

MED134 (Bacteroidetes, Flavobacteriaceae; MED134). All three qualify as moderate

copiotrophs, but, judging by their gene complement, they could be hypothesized to encode

different adaptations serving as response mechanisms to nutrient scarcity. More specifically, the

bacteria encode differences in presence or absence of metabolic pathways – "signature

metabolisms" – that may be used to characterize them in natural communities, suggesting a

deeper understanding of their potential proteome responses to onset of famine could contribute to

interpreting "omics" data from natural communities.

RESULTS

To investigate changes in protein composition in response to different growth phases, the three

marine bacteria were cultivated in nutrient-rich medium with frequent monitoring of growth

(Fig. 1). MED92 grew faster than the other two isolates with a μ_{max} of 1.0 h^{-1} but reached a lower

maximum optical density ($OD_{600} = 0.72$; 8 h incubation). For MED193 in rich medium μ_{max} was

0.365 h^{-1} and it reached a maximum optical density of $OD_{600} = 1.26$ (22 h incubation). Growth of

6

MED134 was similar to MED193 with a μ_{max} of 0.61 h^{-1}, reaching a maximum optical density OD_{600} = 1.24 (24 h incubation).

Proteomic trends among the three marine isolates. Protein expression profiles from the three isolates were obtained using high throughput Nano LC-MS/MS for samples collected in exponential phase and stationary phase (Fig. 1, Supplementary tables S1-6). The total number of proteins encoded in each genome, identified proteins and differentially expressed proteins are listed in Table 1. Overall, 67-87% of proteins encoded in the genomes were detected. Of the detected proteins, 18-38% changed significantly in relative abundance during transition into stationary phase. MED92 and MED193 had larger proportions of differentially abundant proteins (33% and 28% respectively) than MED134 (18%); MED134 on the other hand had the highest proportion of detected proteins (87%). The stable proteins, *i.e.* proteins neither significantly increasing nor decreasing during transition into stationary phase, made up 37%, 39% and 61% of the MED92, MED193 and MED134 proteomes, respectively, in exponential phase, while the same proteins made up 31%, 42% and 61% of the proteomes in stationary phase.

General overview of functional categories among isolates. The detected proteins were classified into 28 top-level functional categories in SEED (25), and the expression patterns were compared between growth phases and among isolates at the different levels of the SEED hierarchy (Fig. 2 and Supplementary table S4-S6). The proteomes of all three isolates changed substantially during the transition from exponential growth into stationary phase, but to different extents. The strongest response was found in MED92 followed by MED193, while MED134 displayed a markedly less pronounced response than the other two (Fig. 2 and Supplementary table S4). Replicates were generally very similar, but MED92 in stationary phase had somewhat larger variation between replicates than the other conditions and isolates. Transition into

7

stationary phase was associated with a decrease in the most abundant SEED1 category, *Protein metabolism*, plus in *RNA metabolism,* in all three isolates. Concomitantly, the relative abundance of several functional categories – Carbohydrates; *Membrane transport*; *Amino acids and derivatives*; *Fatty acids, lipids and isoprenoids*; *Metabolism of aromatic compounds*; *Phosphorus metabolism* – increased in all three isolates (Fig. 2 and Supplementary table S4). *Virulence, disease and defense* increased in abundance in both MED193 and MED92 while *Motility and chemotaxis* and *Dormancy and sporulation* categories increased only in MED92. *Sulfur metabolism* and *Iron acquisition* increased only in MED193.

Protein metabolism. *Protein metabolism* was the most abundant top-level SEED category in all three isolates in both exponential and stationary phase, but the relative abundance of the category decreased in all isolates during transition into stationary phase (Fig. 2 and Supplementary table S4). The largest part of *Protein metabolism* was made up of *Protein biosynthesis* (ribosomal proteins, tRNA aminoacylation proteins and other proteins involved in translation) totaling a few percent to several tens of percents of the proteomes (Supplementary tables S5 and S6). The decrease of *Protein biosynthesis* during transition into stationary phase was also reflected in how ribosomal proteins and other translation-related proteins dominated the lists of the top 50 most abundant in exponential phase but were absent from the corresponding list in stationary phase (Fig. 3).

Membrane transport. Proteins in the Membrane transport SEED category occupied a fairly large proportion of the proteomes in both phases of all three isolates (Fig. 2 and Supplementary table S4). To investigate in further detail the response of transporters to growth phase progression, we performed a separate annotation of the three organisms with respect to transporter classes, subclasses and families/superfamilies, the three levels of the hierarchical TC

system (26). This allowed the classification of threefold more transporters in MED92 (from 134

in SEED Membrane transporters to 420 in TCDB) and twofold more in MED193 (168 to 432)

and MED134 (140 to 321) (Table 2). Abundances of proteins classified in TCDB ranged from

around 12% in exponential phase for all three isolates, to 18% in MED92, 14% in MED193 and

14% in MED134 in stationary phase, compared with single digit percentages of the SEED

classified membrane transporters (Supplementary table S4). Around 70 proteins in the SEED

Membrane transport category were not found in the TCDB classification.

The number of transporters encoded in each genome differed substantially between

strains, with MED92 and MED193 encoding almost double the number of transporter genes as

MED134 (497 and 593 respectively compared to 295) (Table 2). Furthermore, in terms of the

number of differentially abundant transporters, MED92 and MED193 displayed a much clearer

response to growth phase change than MED134. Five times as many transporters were

significantly up in stationary phase in MED92 and MED193 compared with MED134 (60 and 62

in MED92 and MED193 respectively compared with 12 in MED134). More transporters were

also down in stationary compared with exponential phase in MED92 (49) and MED193 (64)

compared with MED134 (22).

MED92 displayed the most profound remodeling of the transporter repertoire, in

particular by an almost threefold increase in *Electrochemical potential-driven transporters* plus a

30% increase of *Channels/pores* (Fig. 4, Table 2 and Supplementary tables S7-10). Moreover, in

this isolate, TC-classified membrane transporters as a group grew about 50% (Table 2 and

Supplementary table S1). MED193 also responded distinctively to growth phase transition by

changes in its expressed transporters. *Electrochemical potential-driven transporters*, *Primary

active transporters* and *Transmembrane electron carriers* increased by 30-50%. Transporters in

9

total increased 20% in MED193. *Channels/pores* dominated the relatively stable MED134 transporter proteome (Fig. 4) where none of the individual classes responded more than 20% and TC-classified transporters as a whole increased a mere 10% from exponential to stationary phase.

The *Tripartite ATP-independent periplasmic transporter* (TRAP-T) family increased almost fivefold in MED92, the strongest response of all transporter families in this isolate (Fig. 4 and Supplementary table S7). At the level of individual transporter proteins, a protein annotated as "Probable DctP (Periplasmic C4-dicarboxylate binding protein)" was the most abundant among several with similar annotations (Supplementary table S8). The highest number (19) of transporter proteins increasing during transition into stationary phase in MED92, but also the highest number of decreasing proteins (15), were found in the *ATP-binding Cassette* (ABC) superfamily, which, like the TRAP-T family, expanded substantially (about 2.5-fold; Fig. 4 and Supplementary table S7). Most of the differentially abundant ABC transporters were insufficiently annotated to deduce their exact function, but amino acids appeared among annotations for both up- and down-regulated proteins in stationary phase, while two cobalt- and vitamin B12-associated proteins appeared among the down-regulated and phosphorus and phosphate was seen in annotations of up-regulated proteins. A third abundant transporter family in MED92 was the *General Bacterial Porin* (GBP) family, which maintained relatively stable relative abundances (Supplementary table S7).

Also in MED193 the TRAP-T and ABC transporter families increased during the transition into stationary phase, both in terms of relative abundance and as number of proteins that were significantly more highly expressed in stationary compared with exponential phase (Fig. 4 and Supplementary table S7). The majority of differentially abundant TRAP-T transporters in MED193, both increasing (8) and decreasing (3) during transition into stationary

10

phase, had annotations suggesting transport of dicarboxylic acids (Supplementary table S10). Among the 176 detected ABC transporters in MED193 (34 up, 29 down in stationary phase), several indications of potential transport substrates could be gleaned: Peptides, amino acids and polyamines were generally up, while sugar transporters and, similar to MED92, cobalt/B12-associated transporters were down. Again similar to MED92, the GBP family was abundant but relatively stable between growth phases in MED193.

MED134 differed markedly from MED92 and MED193 with respect to changes in expression of membrane transporter across growth phases. In MED134, neither TC-classified transporters as a whole, nor any particular class of transporters, increased substantially upon entering stationary phase, and the number of differentially abundant transporters was low (Table 2). Moreover, there was a larger number of proteins that decreased (22) than increased (12) during transition into stationary phase. Transporters in MED134 were dominated by the *Channels/pores* class, which grew somewhat in abundance (30 %) (Fig. 4 and Table 2).

Carbohydrate and related metabolisms. *Carbohydrate metabolism* was one of the most abundant SEED categories in all three isolates (Fig. 2). As a category it increased from exponential to stationary phase in all three isolates (Supplementary table S4). More than 80 proteins increased from exponential to stationary phase, both in MED92 and MED193, while only slightly more than 30 decreased. In MED134, 28 *Carbohydrate metabolism* proteins increased and five decreased. At the second level of the SEED classification, the four categories that were behind most of the proteome in *Carbohydrate metabolism* also contained the majority of proteins that significantly changed in abundance during growth phase transition: *Central carbohydrate metabolism*; *Fermentation*; *One-carbon metabolism*; and *Organic acids* (Supplementary table S5). While this was generally true for all three isolates, the magnitude of

11

responses differed substantially. Furthermore, the differences in metabolism between the three

isolates were reflected in distinct patterns at the level of individual proteins.

All-important steps in glycolysis were detected in all three isolates (Fig. 5). In MED92

several glycolysis enzymes, including the key enzyme of the standard Embden–Meyerhof–

Parnas (EMP) pathway, phosphofructokinase, increased significantly during transition into

stationary phase (Fig. 5 and Supplementary table S1). The MED193 genome does not encode

phosphofructokinase in EMP (Supplementary table S2), instead, it uses the Entner-Doudoroff

(ED) pathway. We detected the complete ED pathway at stable levels except the enzymes

phosphogluconolactonase and phosphoglycerate mutase (Supplementary table S2). Also in

MED134, glycolysis (EMP) enzymes remained largely unchanged during entry into stationary

phase (Fig. 5 and Supplementary table S3). Several enzymes in the pentose phosphate pathway

increased in MED134 during transition into stationary phase. In particular, all enzymes involved

in synthesis of ribose-5-phosphate – including the decarboxylating step catalyzed by 6-

phosphogluconate dehydrogenase – increased.

Both MED92 and MED193 exhibited striking patterns of increases of proteins in the the

first half of the TCA cycle during transition into stationary phase – leading to synthesis of 2-

oxoglutarate, a key metabolite in regulation of carbon and nitrogen metabolism (27, 28) (Fig. 5).

The upregulation of the first half of the TCA cycle was accompanied by several proteins being

down regulated in the second half in both MED92 and MED193. In MED134, no enzymes in the

TCA cycle were significantly differentially abundant between growth phases.

In MED92, isocitrate lyase and malate synthase, the enzymes in the glyoxylate shunt – a

bypass of the downstream steps from isocitrate, generally utilized for subsistence on acetate and

other low molecular weight carbon compounds – also increased. This was accompanied by an increase in stationary phase of phosphoenolpyruvate (PEP) carboxylase – a key anaplerotic CO_2-fixation enzyme – suggesting replenishment of TCA cycle intermediates was an important process in stationary phase (Fig. 5 and Supplementary table S1). Three other proteins involved in C_2-compound metabolism via acetyl-CoA – β-ketothiolase, acetyl-CoA acetyltransferase and a protein annotated as uncharacterized in the genome, but classified as a acetoacetyl-CoA reductase in SEED – increased significantly and reached abundances of up to a few percent (β-ketothiolase) (Fig. 5 and Supplementary table S1). Their increase contributed substantially to the more than twofold increase of the second-level SEED categories *Organic acid metabolism* and *One-carbon metabolism*; and to the almost fivefold increase of the *Fermentation* category. Several other proteins in the three categories also increased during transition to stationary phase, while few decreased (Supplementary table S5). Interestingly, several enzymes involved in acetyl-CoA synthesis from ethanol and pyruvate increased during transition into stationary phase (Fig. 5 and Supplementary table S1). In addition to the acetyl-CoA acetyltransferases, we also detected significant increases in two key enzymes involved in polyhydroxybutyrate (PHB) synthesis: acetoacetyl-CoA reductase and polyhydroxyalkanoic acid synthase (Fig. 5 and Supplementary table S1).

MED193 does not encode the key glyoxylate shunt enzyme isocitrate lyase. However, the ethylmalonyl-CoA pathway – recognized as an alternative to the glyoxylate shunt (29) – is encoded in the MED193 genome. We detected the key CO_2-fixing enzyme in the ethylmalonyl-CoA pathway – crotonyl-CoA reductase – at stable relative abundance between growth phases (Fig. 5 and Supplementary table S2). Furthermore, we did not observe signs of changes in other enzymes involved in anaplerotic CO_2-fixation in MED193. Like in MED92, the second level

13

SEED categories *Fermentation*; *One-carbon metabolism*; and *Organic acids* increased in abundance in MED193, though moderately, during transition into stationary phase. Furthermore, they contained more significantly increasing proteins than decreasing (Supplementary table S5). Similar to in MED92, we detected significant increases for two key enzymes involved in polyhydroxybutyrate (PHB) synthesis: acetoacetyl-CoA reductase and polyhydroxyalkanoic acid synthase (Fig. 5 and Supplementary table S2). Interestingly, in MED193, eight components of carbon monoxide dehydrogenase, plus three maturases for the enzyme, increased significantly during transition into stationary phase (Supplementary table S2); none of these proteins were detected in the other two strains.

In MED134 – in which we did not detect any differentially abundant proteins in the TCA cycle – isocitrate lyase in the glyoxylate shunt decreased in abundance during transition into stationary phase (Fig. 5 and Supplementary table S3). We detected no other signs of upregulation of proteins involved in subsistence on C_2-compounds. Instead, the *Polysaccharides* and *Monosaccharides* second level SEED categories contained larger numbers of significantly increasing proteins: five in both categories, compared with no decreasing proteins in *Monosaccharides* and only two in *Polysaccharides*. Moreover, both categories reached higher relative abundance in MED134 than they did in the other two strains. The *Polysaccharide* category increase was mostly due to enzymes involved in glycogen synthesis. Genes encoding the three enzymes required in synthesis of ADP-glucose (EC 2.7.7.27), polymerisation of ADP-glucose (EC 2.4.1.21) and branching the polymer into glycogen (EC 2.4.1.18) respectively, were all found to significantly increase during transition into stationary phase (Fig. 5 and Supplementary table S3). The increase of genes encoding enzymes categorized in the *Monosaccharide* category was mostly due to an increase of all enzymes in ribose synthesis – *i.e.*

the pentose phosphate pathway (PPP) – starting from glucose (Fig. 5). In particular we detected an almost doubling of the decarboxylating enzyme, 6-phosphogluconate dehydrogenase, that catalyzes the conversion of the C_6 sugar 6-phospho-D-gluconate to the C_5 sugar D-ribulose-5-phosphate, a reaction that is not reversible. The enzyme responsible for conversion of D-ribose-5P to phosphoribosylpyrophosphate, the entry point to nucleotide synthesis, decreased during transition from exponential to stationary phase. Similarly, no enzyme in nucleotide synthesis increased during transition from exponential to stationary phase. Instead, the pentose phosphate enzyme transaldolase – catalyzing the equilibrium reaction that is the entry point to glycolysis for pentose utilization – increased significantly during transition from exponential to stationary phase (EC 2.2.1.2, Fig. 5). The key anaplerotic CO_2-fixation enzyme, PEP carboxylase, was detected in MED134, at low abundance with no signs of differential expression (Supplementary table S3). We did, however, observe a significant increase of another anaplerotic enzyme, pyruvate carboxylase, during transition into stationary phase (Supplementary table S3).

Six components out of eight detected of ATP synthase decreased roughly twofold in MED134 (Supplementary tables S3 and S5). In MED92 and MED193 several ATP synthase components decreased, but few significantly (one and two in MED92 and MED193, respectively) (Supplementary tables S1-2). In MED92 an ATP synthase annotated as V-type in SEED increased. The SEED annotation indicates that the protein was involved in ATP-dependent pumping of protons, instead of proton gradient-dependent ATP synthesis.

Phosphorus and nitrogen metabolism. Proteins involved in phosphorus metabolism were detected in high relative abundances in all three isolates in both growth phases (Fig. 6). Phosphorus metabolism increased substantially during transition into stationary phase in MED92 (nine fold) but also in MED193 and MED134 (three- and twofold respectively) (Supplementary

15

table S4). The periplasmic phosphate-binding protein of the phosphate ABC transporter increased fourfold in MED92 and MED193 and was the most abundant phosphorus-associated protein in both isolates, while it was relatively rare in MED134 (Supplementary tables S5-7). In the latter it also decreased during growth phase transition.

In MED92, 12 proteins involved in phosphorus metabolism increased during transition into stationary phase, while only five decreased. Nearly all proteins that increased were involved in sensing phosphorus, regulating and performing phosphorus transport (Supplementary table S1). In MED193, in addition to these processes, also alkylphosphonate utilization was important, including severalfold increases in the protein products of the *phnGHIJN* genes that encodes subunits of the carbon-phosphorus lyase enzyme together with phosphonate ABC transporter components (Supplementary table S2). In MED134, three out of four significantly increasing proteins in the phosphorus metabolism category were alkaline phosphatases (Supplementary table S3).

Interestingly, proteins involved in nitrogen metabolism did not, in any of the three isolates, reach nearly the same relative abundances as phosphorus metabolism proteins and most nitrogen metabolism-related proteins remained stable across growth phases.

Other metabolisms. Besides the metabolisms described above, a few other top level SEED categories contained interesting patterns. In MED193 and MED134, the *Amino acids and derivatives* category contained a higher number of proteins significantly increasing than decreasing in relative abundance during transition into stationary phase, while almost equal numbers increased as decreased in MED92. In all three isolates the relative abundance of the category as a whole increased (Fig. 2 and Supplementary table S4). Some of the most abundant

proteins significantly more expressed in stationary phase were amino acid ABC transporters (MED92 and MED193), but also enzymes involved in amino acid degradation were abundant, especially leucine dehydrogenase in MED92 (Supplementary tables S1-2). In MED134, proteins in amino acid metabolism that responded to growth phase transition all had very low relative abundances.

In addition, in MED92, the expression of almost 30 proteins involved in flagellar motility increased significantly upon entry into stationary phase, without reaching high abundances (Supplementary table S1 and S5). In MED134, catalase-peroxidase increased four fold and reached relative abundances of roughly one percent of the entire proteome in stationary phase (Supplementary table S3). Finally, in MED92, two proteins associated with dormancy through persister cells increased substantially during transition into stationary phase: a cell division inhibitor that nearly doubled and a ribosome modulation factor (sevenfold increase) (Supplementary table S1). No proteins involved in dormancy were induced in the other two isolates.

Uncharacterized proteins. In all three isolates we detected a large number of proteins that were not classified in SEED, including several that responded significantly to growth phase change, mostly by increasing during transition into stationary phase (Supplementary table S4). Intriguingly, the isolate with the smallest genome of the three studied bacteria, MED134, had the largest number of non-SEED classified proteins (821 out of 2852 proteins, 29%, compared with 18% and 15% respectively for MED92 and MED193). Moreover, large proportions of the non-SEED classified proteins had names indicating they were products of putative open reading frames. In MED92, 485 out of 668 proteins not classified in SEED contained the word "putative" in their names; in MED193, 490 out of 691; and in MED134, 615 out of 821 did (Supplementary

17

tables S1-S3). The uncharacterized proteins, both in their respective genome annotation and in our SEED annotation, summed up to approximately 10% of the abundance of proteomes in stationary phase, while all proteins with "putative" in their names – disregarding their SEED classification and including some with partial annotations – summed to 20-30% of stationary phase proteomes and slightly less in exponential phase.

DISCUSSION

Detection of high proportions of proteomes. Proteomics has developed rapidly from 2D gel electrophoresis with protein spot excision, to the shotgun isoelectric-focusing fractionation followed by nano-LC MS/MS methodology used here (30). At the heart of this development has been an increase in the number of detectable proteins (31, 32), especially apparent for membrane proteins and low abundance proteins (33). The increase has been so rampant that it may alter the general perception of the dynamics of protein expression in microbes. A few years ago it was widely believed that bacteria that readily respond to changes in growth conditions had a highly dynamic proteome, with a relatively small fraction of the entire proteome expressed during most growth conditions. As an example, 1200-1400 proteins were detected in *Ruegeria pomeroyi* DSS-3 – a member of the Roseobacter clade, like MED193 – corresponding to <50% of the theoretical proteome (24). In contrast, we detected between 67% and 87% of the protein coding genes in the genomes of the bacteria studied here. This suggests that a grand majority of proteins in marine bacteria are expressed even in such a uniform environment as a rich medium batch culture. However, the finding that the organisms with the larger genomes of the three expresses a smaller proportion of their proteome, suggests that there appears to be some truth to the common wisdom of larger genomes and proteomes having a more dynamic expression profile than smaller.

Growth and ecological specialization. Dynamic expression of genes and proteins is expected from copiotrophs, heterotrophs that are characterized by a feast and famine strategy involving proteome responses to nutrient pulses. However, the dichotomy between oligotrophs and copiotrophs is likely a simplification. Lauro et al. took this to heart in their 2009 study of trophic strategies in marine bacteria (8), by placing marine bacteria not only on a continuum from extreme oligotrophs to extreme copiotrophs but projecting multiple factors pertaining to trophic strategy on a two-dimensional plane. The considerable differences in both growth characteristics and protein expression between three copiotrophs we detect here, in line with Lauro *et al.'s* analysis, suggests that much can indeed be understood in terms of copiotrophs *vs.* oligotrophs, but also that, in the details, there are many ways of being a copiotroph.

Several functional categories increase at the expense of protein metabolism during transition into stationary phase. Already at the level of the top categories of the SEED classification, it was clear that the proteomes of the three isolates changed profoundly during transition from exponential into stationary phase (Table 2). Several important categories increased in abundance in all three isolates and contained more proteins that significantly increased than decreased during transition into stationary phase. This increase was largely at the expense of *Protein metabolism*, the most abundant of the categories (Fig. 3). In the face of diminishing concentrations of limiting nutrients it thus appears that the relative role of protein, DNA and RNA synthesis becomes less important, and that the importance of effective resource utilization increases. At this high level, the three isolates thus exhibited a shift from the core activities of cell division and growth expected during exponential growth (6, 16, 34), to proteins involved in effectively scavenging nutrients and a wider array of metabolisms in stationary phase(24, 35). This suggests that proteome rearrangements are common parts of the adaptive

19

strategies of marine heterotrophs from different parts of the bacterial phylogeny. With the exception of oligotrophs – like members of the SAR11 clade – we expect such differences to be typical of many marine heterotrophs.

Extensive remodelling of membrane transporters in the Proteobacteria, more stable expression in the Flavobacterium. Although the overall responses of the three isolates were broadly similar, in the specifics, there were clear differences. This was particularly evident in the membrane transporters and carbon and energy metabolisms. Membrane transporters represent important parts of the dynamic proteome both in proteomic analyses (3, 23) and analyses of transcriptomes (36, 37). Moreover, transporters respond to changes in nutrient concentrations and do so in a way that is dependent on the ecological strategy of the organism (8, 38). Because of their importance, we undertook a separate classification of the transporter proteins in the three isolates following the TCDB hierarchical classification (39). This additional annotation effort added substantial information to the analysis, highlighting the importance of choice of databases for annotation and that one database may not serve all purposes.

Our study, like several earlier based both on proteomes and transcriptomes (24, 40, 41), indicates that transporters are important parts of the response of individual isolates to changes in nutrient concentrations. The two Proteobacteria (MED92 and MED193) underwent extensive remodeling of their respective transport proteomes. Moreover, the response takes two shapes, with one being an overall increase in abundance of transporters (Table 2), likely as a reaction to the generally lower nutrient concentrations that induces stationary phase growth in bacteria after depletion of nutrients during exponential phase. The second type of response we detected, were significant increases and decreases of specific transporters both between and within TC superfamilies and families (Table 2 and Fig. 4). We thus observe extensive taxon-specific

20

J Preprints

remodeling of the transport proteome as a response to shifts in relative accessibility of different compounds.

The most abundant transporters in the two Proteobacteria were the primary active transporters, particularly the ABC transporters. ABC transporters transport a wide variety of substrates, carbohydrates, amino acids, vitamins, polyamines, oligopeptides, phosphorus and metal compounds (3, 42, 43). Another transporter family displaying a clear response to growth phase transition in MED92 and MED193 was the TRAP-T transporters – important transporters of diverse carboxylic acids in many bacteria (44, 45). TRAP-T transporters increased substantially during transition into stationary phase, suggesting a potential connection to the increase of C_2/C_3-compound metabolism in the two Proteobacteria. In MED134 we did not detect a similar reflection of changes in its carbon metabolism in the transporter proteome. Overall, MED134 encodes fewer transporters than the other two isolates, but has a higher number of ion channels than the Proteobacteria. Particularly important are the OmpA-OmpF porin family and the outer membrane receptor family.

Differences in central metabolism. If the dynamics among transporter proteins were expected, the dynamics displayed by central metabolism in the three isolates was perhaps more surprising. At least superficially, the Proteobacteria (MED92 and MED193) were more similar to each other in terms of expression pattern than either of them were to the Flavobacterium (MED134). The most striking similarity was an increase of the enzymes in the first half of the TCA cycle – leading to synthesis of 2-oxoglutarate, a key building block in synthesis of certain amino acids (47) – during transition into stationary phase, while the second half remained stable (Fig. 5 and 6). In the details, however, MED92 and MED193 appeared quite distinct from each other. During transition into stationary phase we observed, in MED92, a pattern suggestive of a sugar-starved

organism having to rely on low molecular weight carbon compounds, specifically C_3 compounds like pyruvate and C_2 compounds like acetate and ethanol. We observed an increase of enzymes involved in ethanol to acetyl-CoA oxidation, all glycolysis enzymes involved in conversion of pyruvate to acetyl-CoA, the glyoxylate shunt and PEP carboxylase (Fig. 5). The combination of the glyoxylate shunt and PEP carboxylase is particularly powerful by the dual action of bypass of decarboxylation in the TCA cycle and induction of carboxylation, thus limiting release of carbon as CO_2 and inducing anaplerotic fixation of CO_2. Carbon is thus saved for synthetic purposes. Surprisingly, we did not detect a similar increase in the enzymes of the ethylmalonyl-CoA pathway in MED193, nor did we observe an induction of acetyl-CoA synthesis from pyruvate or ethanol (Fig. 6). In fact, the carboxylating enzyme in the ethylmalonyl-CoA pathway – crotonyl-CoA reductase – significantly decreased during transition into stationary phase. Instead, we observed a clear increase in several components of carbon monoxide dehydrogenase. MED193 does thus not appear synthetically constrained by a lack of carbohydrates during transition into stationary phase. MED134 was apparently even less constrained by reduced access to carbohydrates. The key glyoxylate shunt enzyme decreased and PEP carboxylase was stable during transition into stationary phase and MED134 hence showed no signs of having to restrict loss of carbon. Furthermore, one of the most conspicuous increases in MED134 carbon metabolism was increase in all enzymes involved in ribose synthesis. In particular, the decarboxylating enzyme 6-phosphogluconate dehydrogenase that turns a hexose into a pentose with loss of CO_2, increased, providing further evidence that MED134 was not constrained by low carbohydrate concentrations (Fig. 7).

Based on changes in abundance of enzymes in energy and central carbon metabolism we can thus place the three isolates on a scale of apparent increasing shortage of carbohydrates,

resulting in various degrees of need to economize on reduced carbon compounds. MED134 appeared to have sufficient access to carbohydrates; MED193 displayed no clear signs of shortage of carbohydrates except for an increased reliance on CO as an energy substrate while MED92 appeared to turn to subsistence based primarily on C_2 and C_3 compounds. By and large, much of this is in line with what is known to characterize these organisms. MED92 has been described as preferentially growing on short carbon molecules but not sugars (48), Roseobacter clade species, like MED193, are known to oxidize CO (49, 50) while Flavobacteria, like MED134, have been noted for their appetite for polysaccharides (51, 52). Our proteomic analyses thus highlight the molecular details of these different responses.

Storage polymer synthesis. In the context of the above discussed differences in carbon and energy metabolism, it is interesting to note that all three appeared to devote resources to storage of carbon in polymers, as a strategy during transition into stationary phase. While the overall strategy and potential purpose appears similar over the three isolates, the details were not. The Proteobacteria, MED92 and MED193, increased enzymes involved in synthesis of the fatty acid polymer PHB while the Flavobacterium increased enzymes involved in glycogen synthesis. In both MED92 and MED193, three acetyl-CoA acyltransferases together with acetoacetyl-CoA reductase and polyhydroxyalkanoic acid synthase were found to increase (Supplementary tables S1 and S2). While acetyl-CoA acyltransferases are involved in many C_2 processes, both anabolic and catabolic, the induction of acetoacetyl-CoA reductase and polyhydroxyalkanoic acid synthase suggests that synthesis of the storage molecule PHB was an important part of change in metabolism in the two Proteobacteria. None of this was visible in MED134. Instead, indications of an increase of glycogen synthesis were present in the form of increase of a glycogen synthase, 1.4-alpha-glucan branching enzyme and glucose-1-phosphate adenylyltransferase during

23

transition into stationary phase (Supplementary table S3). Our findings of increases in polymer synthesis are in line with earlier evidence of PHB and glycogen synthesis in bacteria growing on acetate and sugars respectively, during feast and famine growth conditions that has been particularly noted by research into bioreactor applications where bacterial storage reduces the effectiveness of certain process (53-55). That heterotrophic bacteria increase their expression of enzymes involved in storage compound synthesis during transition into stationary phase, as we observe here, is interesting as the underlying processes may influence the general kinetics of carbon storage and release also in natural bacterial communities under changing environmental conditions.

It is interesting to note the differences among the three isolates in growth characteristics (Fig. 1) in light of energy and carbon metabolism in general, and the induction of polymer synthesis in particular. MED92 is by far the quickest of the three to first enter exponential growth phase, deplete its resources and enter stationary phase. It is also the bacterium with the strongest responses both in terms of general increases over categories and in terms of the number of differentially abundant proteins (Fig. 2). When it enters stationary phase it does so at a much lower cell density than the other two strains, and thus potentially at a stage when lower amounts of nutrients are bound in cells. MED92 hence appears to need higher concentrations of nutrients to sustain exponential growth and to replace cell growth and division with storage of carbon for leaner days at an earlier point of time than the other two isolates. There are differences between MED193 and MED134 too, especially in that the former is slow to enter exponential phase. In contrast, it exits exponential phase and enters stationary quicker than MED134. As the two isolates also have quite different metabolic signatures in carbon metabolism, in particular when it

24

concerns synthesis of storage polymers, it is, however, difficult to interpret these relatively subtle differences in growth.

Phosphorus metabolism. Another example of a similarity in metabolic purpose and general strategy between the three isolates, but with differences in the details, concerns phosphorus utilization. All three isolates showed signs of an increased competition for phosphorus compounds by increasing the expression of mainly transporters (Supplementary table S5). We did not detect any signs of a corresponding shortage of nitrogen in any of the isolates, suggesting the growth medium was underbalanced in phosphorus to nitrogen in comparison with the stoichiometry of all isolates. The three phylogenetic lineages that our isolates represent have been noted for their differences in phosphorus uptake and utilization (38). In particular, Roseobacter clade members are known to be able to utilize alkylphosphonates (38, 56), while the other two are not. This was clear also in our data, as nine enzymes involved in alkylphosphonate utilization increased significantly during transition into stationary phase and the category as a whole increased more than threefold (Supplementary tables S1-3 and S5-6).

CONCLUSIONS

Application of understanding gained from detailed studies of environmentally relevant model organisms is important for the interpretation of community data such as nucleotide sequences – metagenomics and metatranscriptomics – or high throughput proteomic profiles – metaproteomics. As we show here by comparing the proteomic profiles of three marine bacteria as functions of growth phase transition, this approach has the potential to reveal similarities and differences both at the level of general trophic strategy and at the level of metabolic detail seen as the result of evolutionary contingency. At a very general level, the three isolates responded

similarly to transition from exponential into stationary phase, *e.g.* by increased abundances of enzymes involved in synthesis of storage polymers. In the details, however, the three isolates displayed characteristic signatures in their proteomic profiles in particular with respect to apparent carbon and energy sources, suggesting the induction of signature metabolisms in each isolate. MED92 increased enzymes involved in energy conversion and storage based on short-chained carbon molecules – acetyl-CoA metabolism based on C_2 and C_3 compounds – coupled with anaplerotic CO_2 fixation. MED193 appears to store carbon and energy as a fatty acid polymer (PHB) like MED92, but relies to some extent on CO-oxidation as an energy source. Lastly, MED134, although displaying a less pronounced response to growth phase change than the Proteobacteria, appears to rely on sugars both for its immediate energy requirements and for storage. The ability of high throughput proteomics to detect these differences in response between organisms in a qualitative way – by detecting the presence of signature metabolisms – but also in a quantitative way – by detecting differential expression between conditions – provides important validation for the application of the methodology but also, and more importantly, for interpretation of proteomic data from natural microbial communities.

MATERIALS AND METHODS

Bacterial growth condition. The Gammaproteobacterium *Neptuniibacter* sp. strain MED92, Alphaproteobacterium *Phaeobacter* sp. strain MED193 and Flavobacterium *Dokdonia* sp. strain MED134 were cultured with peptone and yeast extract containing Bacto Marine Broth (DIFCO 2216; DIFCO, Lawrence, KS, USA) medium. Cultures were grown in 20 ml of marine broth overnight. Hereafter 1 ml of overnight grown culture was transferred into 300 ml of fresh marine broth medium in triplicates. All the bacterial cultures were incubated on a rotary shaker at 142 rpm at room temperature and the bacterial growth was measured by monitoring the optical

26

density at 600 nm (OD_{600}) for 34 h. Protein samples were collected at both exponential and stationary phase. Bacterial cells were harvested by centrifugation at 4000 rpm for 20 min at 4ºC using Beckman Avanti J-25 (Rotor Beckman JA-14). Cell Pellets were washed three times with 1X phosphate buffered saline (PBS) solution (137 mM NaCl, 2.7 mM KCl, 10 mM Na_2HPO_4, 2 mM KH_2PO_4 (Sigma Chemical Co., St. Louis, Mo) and pH = 7.4). Samples were stored at -80 ºC until protein extraction was performed.

Cell lysis, protein extraction, digestion, and peptide labeling with TMT6plex. Cell pellets were lysed in SDS-lysis buffer pH 7.6 contains 4 % (w/v) SDS, 25 mM HEPES and 1 mM dithiothreitol (DTT) (Sigma Aldrich). Lysates were heated to 95º C for 5 min and samples were sonicated with a sonicator probe to shear DNA. Samples were centrifuged at 14000 g to remove cell debris, the supernatant was collected and protein concentration in the supernatant estimated using the Bio-Rad DC-protein assay (Bio-Rad Laboratories, Hercules, CA). From each sample, 250 µg of total protein were taken and processed according to the FASP (Filter aided sample preparation protocol (57). Peptide concentration was estimated by the DC-protein assay (BioRad Laboratories, Hercules, CA, USA), and 100 µg of peptides from each sample were labeled with TMT6plex (Thermo Fisher Scientific) according to the manufacturer's instructions.

HiRIEF (High resolution isoelectric focusing) separation. After pooling the samples that belong together in each TMT set, each TMT set was cleaned by strong cation exchange solid phase extraction (SCX-SPE, Phenomenex Strata-X-C, P/N 8B-S029-TAK). After drying in a speedvac, the equivalent to 400 µg of peptides of each sample were dissolved in 250 µL of 8 M urea, 1 % pharmalyte (broad range pH 3-10, GE Healthcare, P/N 17-0456-01), and this solution was used to rehydrate the IPG drystrip (pH 3-10, 24 cm, GE Healthcare, P/N 17-6002-44) overnight. Focusing was done on an Ettan IPGphor 3 system (GE Healthcare) ramping up the

voltage to 500 V in one hour, then to 2000 V in two more hours, and finally to 8000 V in six more hours, after which voltage was held at 8000 V for additional 20 h or until 150 kVh were reached. After focusing was complete, a well-former with 72 wells was applied onto each strip, and liquid-handling robotics (GE Healthcare prototype), using three rounds of different solvents (i. milliQ water, ii. 35 % acetonitrile, and iii. 35 % acetonitrile, 0.1 % formic acid), added 50 µL of solvent to each well and transferred the 72 fractions into a microtiter plate (96 wells, PP, V-bottom, Greiner P/N 651201), which was then dried in a SpeedVac.

LC-MS analysis. Prior to each LC-MS run, the LC auto sampler (HPLC 1200 system, Agilent Technologies) dispensed 8 µL of solvent A to the dry HiRIEF fraction (in its micro-titer plate well), mixed by aspirating/dispensing 6 µL ten times, and injected 3 µL into a C18 guard desalting column (Zorbax 300SB-C18, 5x0.3mm, 5µm bead size, Agilent Technologies). We then used a 15 cm long C18 picofrit column (100 µm internal diameter, 5 µm bead size, Nikkyo Technos Co., Tokyo, Japan) installed on to the nano electrospray ionization (NSI) source. Solvent A was 97 % water, 3 % acetonitrile (ACN), 0.1 % formic acid (FA); and solvent B was 5 % water, 95 % ACN, 0.1 % FA. At a constant flow of 0.4 µL/min, the curved gradient went from 2 % B up to 40 % B in 45 min, followed by a steep increase to 100 % B in 5 min, wash for 5 min at 100 % B and re-equilibration. Online LC-MS was performed using a hybrid Q-Exactive mass spectrometer (Thermo Scientific). FTMS master scans with 70,000 resolution (and mass range 300-1700 m/z) were followed by data-dependent MS/MS (35,000 resolution) on the top 5 ions using higher energy collision dissociation (HCD) at 30 % normalized collision energy. Precursors were isolated with a 2 m/z window. Automatic gain control (AGC) targets were 1e6 for MS1 and 1e5 for MS2. Maximum injection times were 100ms for MS1 and 150ms for MS2.

28

The entire duty cycle lasted ~1.5 s. Dynamic exclusion was used with 60 s duration. Precursors with unassigned charge state or charge state 1 were excluded. An underfill ratio of 1 % was used.

Proteomics database search. All MS/MS spectra were searched by Sequest/Percolator under the software platform Proteome Discoverer (PD 1.3, Thermo Scientific) using a target-decoy strategy. Reference databases of the taxonomic groups *Dokdonia* sp. MED134, *Neptuniibacter* sp. MED92, and *Phaeobacter* sp. MED193 were downloaded from uniprot.org on 2012/10/11. Precursor mass tolerance of 10 ppm and product mass tolerance of 0.02 Da were used. Additional settings were trypsin with one missed cleavage; Lys-Pro and Arg-Pro not considered as cleavage sites; carbamidomethylation on cysteine and TMT-10plex on lysine and N-terminus as fixed modifications; and oxidation of methionine as variable modification. Quantitation of TMT-6plex reporter ions was done using an integration window tolerance of 20 ppm. Peptides found at 1 % FDR (false discovery rate) were used by the protein grouping algorithm in PD to infer protein identities. Protein level FDR of the resulting protein lists was estimated using the "picked" protein FDR approach (58).

Statistical analysis of up and down regulation. The protein table exported from PD contains protein ratios (proteins with missing ratios were discarded), which were logged (base 2) in excel, before performing statistical analysis by SAM (Significance Analysis of Microarrays) (http://statweb.stanford.edu/~tibs/SAM/). Response type used was "Two class unpaired", analysis type was standard, t-statistic was used, arrays were not median centered (since PD already carries out a normalization to protein median on the protein table), and the number of permutations was 720 (maximum for 3 VS 3 values). A q-value, or FDR of 5 % was used as significance threshold for up and down regulation.

Order of magnitude approximate abundances were calculated by multiplying the normalized area of a protein – in turn calculated by dividing the area value of each protein as given in Proteome Discoverer by the sum of areas of all proteins in the dataset – with the ratio of each channel to the total of channel readings for that protein.

Annotation. Detected protein sequences were aligned to the M5NR database (59) using BLAST (60) and sequences with hits with bitscores > 50 annotated using in house developed scripts. The BioCyc maps were created by manually selecting proteins matching MetaCyc (61)(reactions from the list of detected proteins and using the Omics paint tool(62). In cases where more than one protein matched the enzyme in MetaCyc, a conservative choice was made by selecting a non-significant before a significant protein, a better annotated (*i.e.* with a meaningful, non-contradictory, annotation in SEED and by the protein name) and a more abundant protein over a less abundant. The TCDB (63) annotation was created manually (26).

FUNDING INFORMATION

ACKNOWLEDGEMENTS

REFERENCES

1.   **Arrigo KR.** 2004. Marine microorganisms and global nutrient cycles. Nature **437:**349-
        355.

2.   **Karl DM.** 2007. Microbial oceanography: paradigms, processes and promise. Nat Rev
        Microbiol **5:**759-769.

3.   **Sowell SM, Wilhelm LJ, Norbeck AD, Lipton MS, Nicora CD, Barofsky DF, Carlson
        CA, Smith RD, Giovanonni SJ.** 2009. Transport functions dominate the SAR11
        metaproteome at low-nutrient extremes in the Sargasso Sea. ISME J **3:**93-105.

4.   **Scanlan DJ, Wilson WH.** 1999. Application of molecular techniques to addressing the
        role of P as a key effector in marine ecosystems. Hydrobiologia **401:**149-175.

5.   **Mills MM, Ridame C, Davey M, La Roche J, Geider RJ.** 2004. Iron and phosphorus
        co-limit nitrogen fixation in the eastern tropical North Atlantic. Nature **429:**292-294.

6.   **Bernhardt J, Weibezahn J, Scharf C, Hecker M.** 2003. *Bacillus subtilis* during feast
        and famine: visualization of the overall regulation of protein synthesis during glucose
        starvation by proteome analysis. Genome Res **13:**224-237.

7.   **Gade D, Stuhrmann T, Reinhardt R, Rabus R.** 2005. Growth phase dependent
        regulation of protein composition in *Rhodopirellula baltica*. Environ Microbiol **7:**1074-
        1084.

8.   **Lauro FM, McDougald D, Thomas T, Williams TJ, Egan S, Rice S, DeMaere MZ,
        Ting L, Ertan H, Johnson J.** 2009. The genomic basis of trophic strategy in marine
        bacteria. Proc Natl Acad Sci U S A **106:**15527-15533.

9.   **Siegele DA, Kolter R.** 1992. Life after log. J Bacteriol **174:**345-348.

32

10.   **Ishihama A.** 1997. Adaptation of gene expression in stationary phase bacteria. Curr Opin Genetics Dev **7:**582-588.

11.   **Lange R, Hengge‑Aronis R.** 1991. Identification of a central regulator of stationary-phase gene expression in *Escherichia coli*. Mol Microbiol **5:**49-59.

12.   **Phillips ZEV, Strauch MA.** 2002. *Bacillus subtilis* sporulation and stationary phase gene expression. Cell Mol Life Sci **59:**392-402.

13.   **Chaiyanan S, Chaiyanan S, Grim C, Maugel T, Huq A, Colwell RR.** 2006. Ultrastructure of coccoid viable but non-culturable *Vibrio cholerae*. Environ Microbiol **9:**393-402.

14.   **Arana I, Muela A, Orruño M, Seco C, Garaizabal I, Barcina I.** 2010. Effect of temperature and starvation upon survival strategies of *Pseudomonas fluorescens* CHA0: comparison with *Escherichia coli*. FEMS Microbiol Ecol **74:**500-509.

15.   **Eymann C, Dreisbach A, Albrecht D, Bernhardt J, Becher D, Gentner S, Tam LT, Büttner K, Buurman G, Scharf C.** 2004. A comprehensive proteome map of growing *Bacillus subtilis* cells. Proteomics **4:**2849-2876.

16.   **Folio P, Chavant P, Chafsey I, Belkorchia A, Chambon C, Hebraud M.** 2004. Two-dimensional electrophoresis database of *Listeria monocytogenes* EGDe proteome and proteomic analysis of mid-log and stationary growth phase cells. Proteomics **4:**3187-3201.

17.   **Strauch MA.** 1993. Regulation of *Bacillus subtilis* gene expression during the transition from exponential growth to stationary phase. Prog Nucleic Acid Res Mol Biol **46:**121-153.

18.   **Jenkins DE, Schultz JE, Matin A.** 1988. Starvation-induced cross protection against
       heat or H_2O_2 challenge in *Escherichia coli*. J Bacteriol **170:**3910-3914.

19.   **Matin A.** 1991. The molecular basis of carbon-starvation-induced general resistance in
       Escherichia coli. Mol Microbiol **5:**3-10.

20.   **Yoon SH, Han MJ, Lee SY, Jeong KJ, Yoo JS.** 2003. Combined transcriptome and
       proteome analysis of *Escherichia coli* during high cell density culture. Biotechnol Bioeng
       81:753-767.

21.   **Sowell SM, Norbeck AD, Lipton MS, Nicora CD, Callister SJ, Smith RD, Barofsky
       DF, Giovannoni SJ.** 2008. Proteomic analysis of stationary phase in the marine
       bacterium "*Candidatus* Pelagibacter ubique". Appl Environ Microbiol **74:**4091-4100.

22.   **Steindler L, Schwalbach MS, Smith DP, Chan F, Giovannoni SJ.** 2011. Energy
       starved *Candidatus* Pelagibacter Ubique substitutes light-mediated ATP production for
       endogenous carbon respiration. PLoS One **6:**e19725.

23.   **Christie-Oleza JA, Pina-Villalonga JM, Bosch R, Nogales B, Armengaud J.** 2012.
       Comparative proteogenomics of twelve Roseobacter exoproteomes reveals different
       adaptive strategies among these marine bacteria. Mol Cell Proteomics **11:**M111.013110.

24.   **Christie-Oleza JA, Fernandez B, Nogales B, Bosch R, Armengaud J.** 2012. Proteomic
       insights into the lifestyle of an environmentally relevant marine bacterium. ISME J
       6:124-135.

25.   **Overbeek R, Begley T, Butler RM, Choudhuri JV, Chuang HY, Cohoon M, de
       Crécy-Lagard V, Diaz N, Disz T, Edwards R.** 2005. The subsystems approach to
       genome annotation and its use in the project to annotate 1000 genomes. Nucleic Acids
       Res **33:**5691-5702.

26.   **Akram N.** 2013. PhD thesis. Linnaeus University, Kalmar, Sweden. From genes to ecological function in marine bacteria.

27.   **Commichau FM, Forchhammer K, Stülke J.** 2006. Regulatory links between carbon and nitrogen metabolism. Curr Opin Microbiol **9:**167-172.

28.   **Huergo LF, Dixon R.** 2015. The emergence of 2-oxoglutarate as a master regulator metabolite. Microbiol Mol Biol R **79:**419-435.

29.   **Erb TJ, Berg IA, Brecht V, Muller M, Fuchs G, Alber BE.** 2007. Synthesis Of C-5-dicarboxylic acids from C-2-units involving crotonyl-CoA carboxylase/reductase: The ethylmalonyl-CoA pathway. Proc Natl Acad Sci U S A **104:**10631-10636.

30.   **Branca RMM, Orre LM, Johansson HJ, Granholm V, Huss M, Pérez-Bercoff Å, Forshed J, Käll L, Lehtiö J.** 2014. HiRIEF LC-MS enables deep proteome coverage and unbiased proteogenomics. Nat Methods **11:**59-62.

31.   **Beck S, Michalski A, Raether O, Lubeck M, Kaspar S, Goedecke N, Baessmann C, Hornburg D, Meier F, Paron I.** 2015. The impact II, a very high resolution quadrupole time-of-flight instrument for deep shotgun proteomics. Mol Cell Proteomics **14:**2014-2029.

32.   **Hebert AS, Richards AL, Bailey DJ, Ulbrich A, Coughlin EE, Westphall MS, Coon JJ.** 2014. The one hour yeast proteome. Mol Cell Proteomics **13:**339-347.

33.   **Gilmore JM, Washburn MP.** 2010. Advances in shotgun proteomics and the analysis of membrane proteomes. J Proteomics **73:**2078-2091.

34.   **Cohen DP, Renes J, Bouwman FG, Zoetendal EG, Mariman E, de Vos WM, Vaughan EE.** 2006. Proteomic analysis of log to stationary growth phase *Lactobacillus plantarum* cells and a 2-DE database. Proteomics **6:**6485-6493.

35

35.   **Bernhardt J, Völker U, Völker A, Antelmann H, Schmid R, Mach H, Hecker M.**
        1997. Specific and general stress proteins in *Bacillus subtilis*–a two-dimensional protein
        electrophoresis study. Microbiology **143:**999-1017.

36.   **Poretsky RS, Sun S, Mou X, Moran MA.** 2010. Transporter genes expressed by coastal
        bacterioplankton in response to dissolved organic carbon. Environ Microbiol **12:**616-627.

37.   **Ottesen EA, Young CR, Eppley JM, Ryan JP, Chavez FP, Scholin CA, DeLong EF.**
        2013. Pattern and synchrony of gene expression among sympatric marine microbial
        populations. Proc Natl Acad Sci U S A **110:**E488-E497.

38.   **Teeling H, Fuchs BM, Becher D, Klockow C, Gardebrecht A, Bennke CM, Kassabgy
        M, Huang S, Mann AJ, Waldmann J, Weber M, Klindworth A, Otto A, Lange J,
        Bernhardt J, Reinsch C, Hecker M, Peplies J, Bockelmann FD, Callies U, Gerdts G,
        Wichels A, Wiltshire KH, Glockner FO, Schweder T, Amann R.** 2012. Substrate-
        controlled succession of marine bacterioplankton populations induced by a phytoplankton
        bloom. Science **336:**608-611.

39.   **Saier MH.** 2000. A functional-phylogenetic classification system for transmembrane
        solute transporters. Microbiol Mol Biol R **64:**354-411.

40.   **Wick LM, Quadroni M, Egli T.** 2001. Short-and long-term changes in proteome
        composition and kinetic properties in a culture of *Escherichia coli* during transition from
        glucose-excess to glucose-limited growth conditions in continuous culture and vice versa.
        Environ Microbiol **3:**588-599.

41.   **Ferenci T.** 1999. Regulation by nutrient limitation Curr Opin Microbiol **2:**208-213.

42.   **Boos W, Eppler T.** 2001. Prokaryotic binding protein-dependent ABC transporters. p 77–
114. *In* Winkelmann G (ed), Microbial Transport Systems. Wiley-VCH, Weinheim,
Germany.

43.   **Morris RM, Nunn BL, Frazar C, Goodlett DR, Ting YS, Rocap G.** 2010.
Comparative metaproteomics reveals ocean-scale shifts in microbial nutrient utilization
and energy transduction. ISME J **4:**673-685.

44.   **Moran MA, Belas R, Schell MA, Gonzalez JM, Sun F, Sun S, Binder BJ, Edmonds
J, Ye W, Orcutt B.** 2007. Ecological genomics of marine roseobacters. Appl Environ
Microbiol **73:**4559-4569.

45.   **Mulligan C, Fischer M, Thomas GH.** 2011. Tripartite ATP-independent periplasmic
(TRAP) transporters in bacteria and archaea. FEMS Microbiol Rev **35:**68-86.

46.   **Alber BE, Spanheimer R, Ebenau-Jehle C, Fuchs G.** 2006. Study of an alternate
glyoxylate cycle for acetate assimilation by *Rhodobacter sphaeroides*. Mol Microbiol
61:297-309.

47.   **Berg JM, Tymoczko JL, Stryer L.** 2012. Glycolysis and gluconeogenesis, p. 425–464.
In Berg JM, Tymoczko JL, Stryer L (ed), Biochemistry, 5th ed, W.H. Freeman and
Company, New York.

48.   **Arahal DR, Lekunberri I, González JM, Pascual J, Pujalte MJ, Pedrós-Alió C,
Pinhassi J.** 2007. *Neptuniibacter caesariensis* gen. nov., sp. nov., a novel marine
genome-sequenced gammaproteobacterium. Int J Syst Evol Microbiol **57:**1000-1006.

49.   **Moran MA, Buchan A, Gonzalez JM, Heidelberg JF, Whitman WB, Kiene RP,
Henriksen JR, King GM, Belas R, Fuqua C, Brinkac L, Lewis M, Johri S, Weaver
B, Pai G, Eisen JA, Rahe E, Sheldon WM, Ye WY, Miller TR, Carlton J, Rasko DA,**

Paulsen IT, Ren QH, Daugherty SC, Deboy RT, Dodson RJ, Durkin AS, Madupu R, Nelson WC, Sullivan SA, Rosovitz MJ, Haft DH, Selengut J, Ward N. 2004. Genome sequence of *Silicibacter pomeroyi* reveals adaptations to the marine environment. Nature **432:**910-913.

50.   **Newton RJ, Griffin LE, Bowles KM, Meile C, Gifford S, Givens CE, Howard EC, King E, Oakley CA, Reisch CR, Rinta-Kanto JM, Sharma S, Sun SL, Varaljay V, Vila-Costa M, Westrich JR, Moran MA.** 2010. Genome characteristics of a generalist marine bacterial lineage. ISME J **4:**784-798.

51.   **Williams TJ, Wilkins D, Long E, Evans F, Demaere MZ, Raftery MJ, Cavicchioli R.** 2013. The role of planktonic *Flavobacteria* in processing algal organic matter in coastal East Antarctica revealed using metagenomics and metaproteomics. Environ Microbiol **15:**1302-1317.

52.   **Xing P, Hahnke RL, Unfried F, Markert S, Huang S, Barbeyron T, Harder J, Becher D, Schweder T, Glöckner FO.** 2014. Niches of two polysaccharide-degrading *Polaribacter* isolates from the North Sea during a spring diatom bloom. ISME J **9**:1410-1422.

53.   **Carta F, Beun JJ, Van Loosdrecht MCM, Heijnen JJ.** 2001. Simultaneous storage and degradation of PHB and glycogen in activated sludge cultures. Water research **35:**2693-2701.

54.   **Dawes EA, Senior PJ.** 1973. The role and regulation of energy reserve polymers in microorganisms polyhydroxybutyrate. Adv Microb Physiol **10:**203-266.

55.   **Zevenhuizen LPTM.** 1981. Cellular glycogen, β-1, 2-glucan, poly-β-hydroxybutyric acid and extracellular polysaccharides in fast-growing species of Rhizobium. Antonie Van Leeuwenhoek **47:**481-497.

56. **Chan LK, Newton RJ, Sharma S, Smith CB, Rayapati P, Limardo AJ, Meile C, Moran MA.** 2012. Transcriptional changes underlying elemental stoichiometry shifts in a marine heterotrophic bacterium. Front Microbiol **3**:159.

57. **Wiśniewski JR, Zougman A, Nagaraj N, Mann M.** 2009. Universal sample preparation method for proteome analysis. Nat Methods **6**:359-362.

58. **Savitski MM, WIlhelm M, Hahne H, Kuster B, Bantscheff M.** 2015. A scalable approach for protein false discovery rate estimation in large proteomic data sets. Mol Cell Proteomics **14:**2394-2404.

59. **Wilke A, Harrison T, Wilkening J, Field D, Glass EM, Kyrpides N, Mavrommatis K, Meyer F.** 2012. The M5nr: a novel non-redundant database containing protein sequences and annotations from multiple sources and associated tools. BMC Bioinformatics **13:**141.

60. **Altschul SF, Madden TL, Schäffer AA, Zhang J, Zhang Z, Miller W, Lipman DJ.** 1997. Gapped BLAST and PSI-BLAST: a new generation of protein database search programs. Nucleic Acids Res **25:**3389-3402.

61. **Caspi R, Billington R, Ferrer L, Foerster H, Fulcher CA, Keseler IM, Kothari A, Krummenacker M, Latendresse M, Mueller LA, Ong Q, Paley S, Subhraveti P, Weaver DS, Karp PD.** 2015. The MetaCyc database of metabolic pathways and enzymes and the BioCyc collection of pathway/genome databases. Nucleic Acids Res **44:** D471-D480.

62. **Karp PD, Latendresse M, Paley SM, Krummenacker M, Ong QD, Billington R, Kothari A, Weaver DS, Lee T, Subhraveti P.** 2015. Pathway Tools version 19.0 update: software for pathway/genome informatics and systems biology. Brief Bioinform [Epub ahead of print.]

39

63.   **Saier MH, Reddy VS, Tamang DG, Västermark Å.** 2014. The transporter

       classification database. Nucleic Acids Res **42**:D251–D258.

TABLE 1. General proteome statistics. Number of proteins encoded in the genome, number of detected peptides, number of detected expressed proteins, protein identification FDR, number of not significantly differentially abundant, number of proteins increasing during transition into stationary phase and number of decreasing proteins. Percentages for the number of detected proteins denote proportions of the genomically encoded proteins; all other percentages are proportions of the detected proteins.

Isolate	Proteins encoded	Detected peptides	Detected proteins	Ident. FDR	Stable proteins	Proteins increasing	Proteins decreasing
MED92	3688	30990	2930 (79%)	1.5%	1830 (62%)	603 (21%)	497 (17%)
MED193	4535	30591	3038 (67%)	1.4%	2015 (66%)	558 (18%)	465 (15%)
MED134	2852	31854	2476 (87%)	0.8%	2018 (82%)	281 (11%)	177 (7%)

TABLE 2. Responses in membrane transporter proteins across growth phases. Number of encoded transporters in genome ("Enc."), proteins detected in our experiments ("Det."), significantly more and less abundant proteins in stationary compared with exponential phase ("Up" and "Down" respectively) and fold change between stationary and exponential ("FC %"). The fold change was based on approximate relative abundances for each class and was rounded to single digit precision, reflecting the approximate nature of the abundances. Transporters identified in TCDB. Color codings same as in Fig. 4.

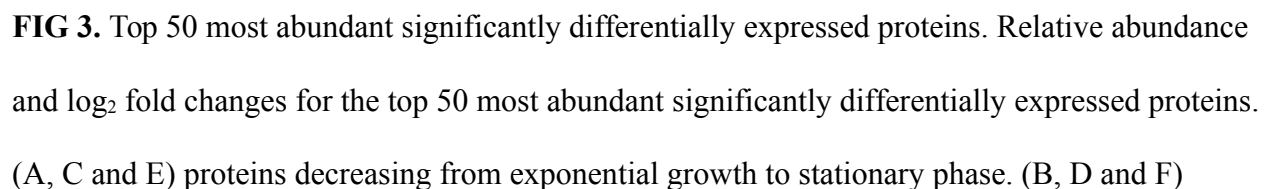| Class	MED92					MED193					MED134				
	Enc.	Det.	Up	Down	FC %	Enc.	Det.	Up	Down	FC %	Enc.	Det.	Up	Down	FC %
Channels/pores	51	43	5	5	30	42	30	6	3	0	78	72	7	4	30
Electrochemical Potential- driven Transporters	157	81	18	15	200	156	66	11	11	40	71	46	1	6	10
Group Translocators	1	1	0	0	-30	1	1	0	0	-10	0	0	0	0	
Incompletely Characterized Transport Systems	22	20	4	2	-30	19	14	1	4	0	41	34	0	1	20
Primary Active Transporters	264	203	33	27	10	369	250	43	46	30	104	98	4	11	-20
Transmembrane Electron Carriers	2	2	0	0	-30	6	2	1	0	50	1	1	0	0	-40
Sums	497	350	60	49	50	593	363	62	64	20	295	251	12	22	10
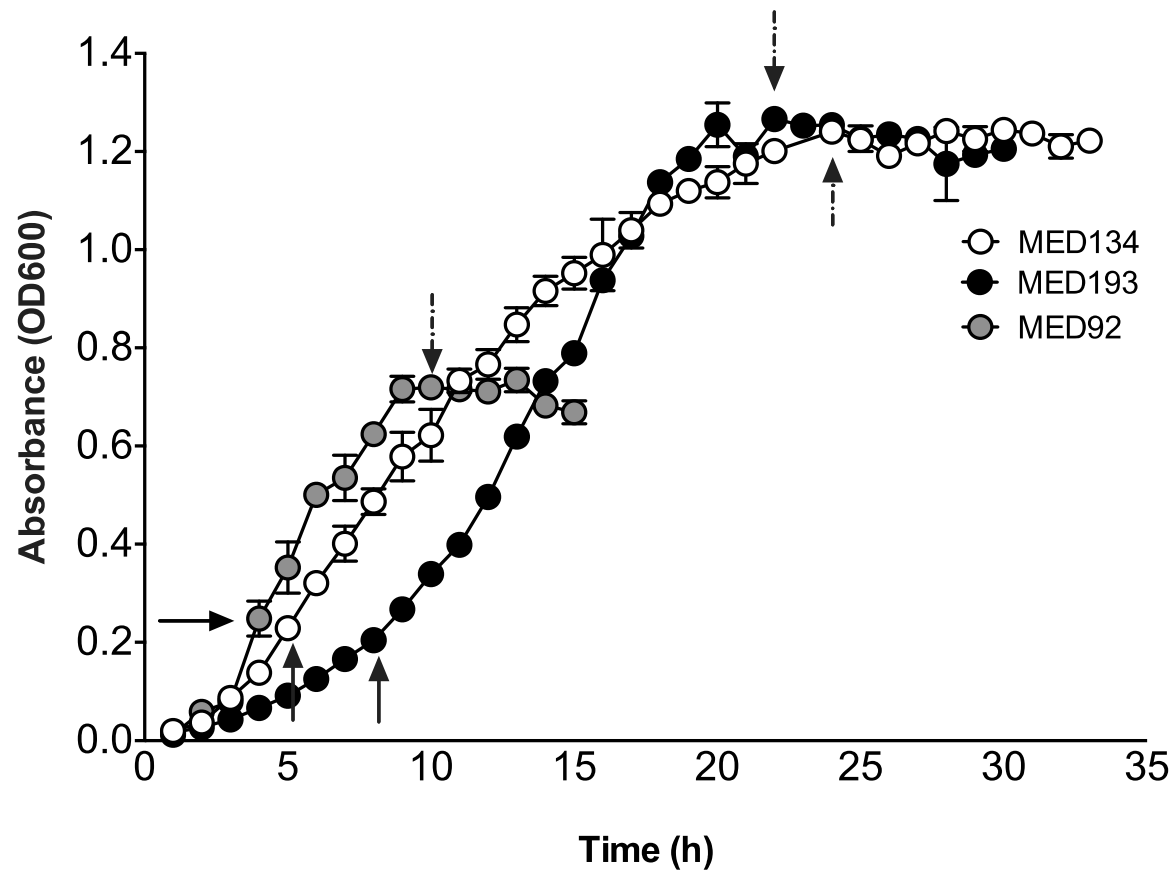
FIG 1. Growth curves of three phylogenetically distinct representatives of marine bacterioplankton in nutrient rich marine broth medium. Cells were harvested for proteomic analysis at the time points indicated by arrows for exponential phase (solid arrows) and stationary phase (hatched arrows) respectively. Error bars denote the standard deviation of three biological replicates. If not visible, error bars are within symbols.

FIG 2. Overall growth phase-associated changes in proteomes. (A, C, E) Relative abundances of detected proteins grouped into top level SEED categories: (A) MED92, (C) MED193 and (E) MED134. The three replicates are shown for exponential phase (open circles) and stationary phase (filled circles). Note the log scale on Y-axes. (B, D, F) Counts (y-axis) of increasing (right-pointing triangles), stable (circles) and decreasing proteins (left-pointing triangles) and relative abundances (size of symbols): (B) MED92, (D) MED193 and (F) MED134. Proteins that belong in more than one category were counted in all. Note that y-axes have been cut at 200; categories that exceed 200 were inserted at 200 with a label denoting the proper count.

FIG 3. Top 50 most abundant significantly differentially expressed proteins. Relative abundance

and log₂ fold changes for the top 50 most abundant significantly differentially expressed proteins.

(A, C and E) proteins decreasing from exponential growth to stationary phase. (B, D and F)

proteins increasing from exponential growth to stationary phase. (A, B) MED92; (C, D)

MED193; and (E, F) MED134. Color codes denote the different functional categories in the

SEED classification, Blue: *Protein metabolism*, Green: *Membrane transporters*, Orange: *Stress*

response, Purple: *Carbon metabolism*, Grey: *Amino acids and derivatives* and Yellow:
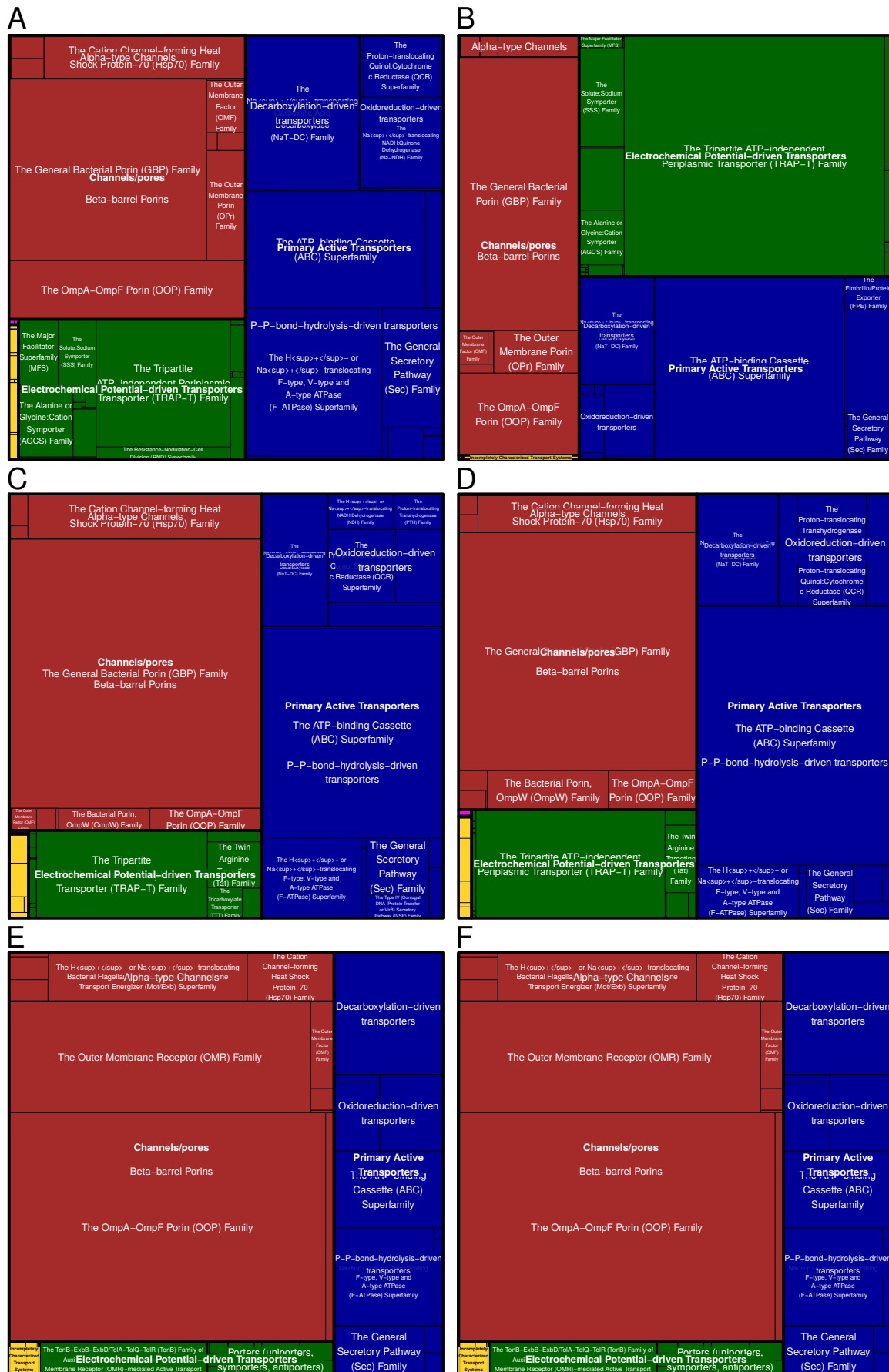
Respiration.

48

FIG 4. Changes in relative proportions of membrane transporter categories across growth phases. (A, C, E) Exponential phase in (A) MED92, (C) MED193 and (E) MED134. (B, D, F) Stationary phase in (B) MED92, (D) MED193 and (F) MED134. The areas of rectangles are proportional to relative abundances of categories at the three levels of the TC classification. Top-level categories are denoted with colored rectangles and labels in bold; second level categories are normal font labels spanning several rectangles; and third level categories have labels inside rectangles. Transporter identification according to TC categories.
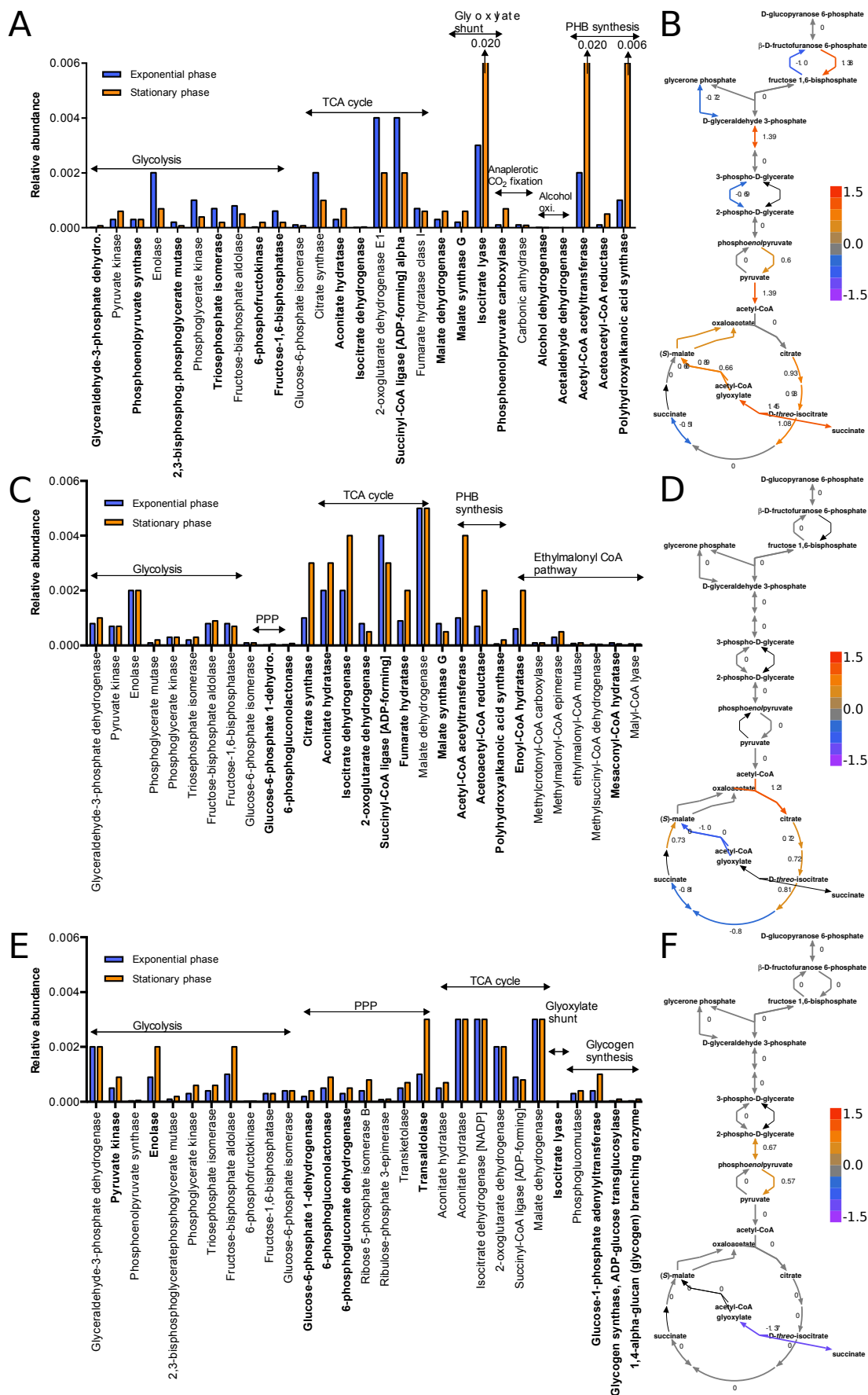
51

FIG 5. Carbon metabolisms. (A, C, E) Relative abundances, averaged over triplicates for each growth phase, for enzymes in five important carbon metabolisms in (A) MED92, (C) MED193 and (E) MED134. Significantly differentially abundant proteins have names in bold font. (B, D, F) Glycolysis (EMP), TCA cycle and glyoxylate shunt BioCyc pathways in (B) MED92, (D) MED193 and (F) MED134. Heatmap indicating $\log_2$ fold changes of stationary phase in relation to exponential phase. Grey arrows indicate stable, *i.e.* not significantly differentially abundant proteins. Thin black arrows indicate non detected proteins.
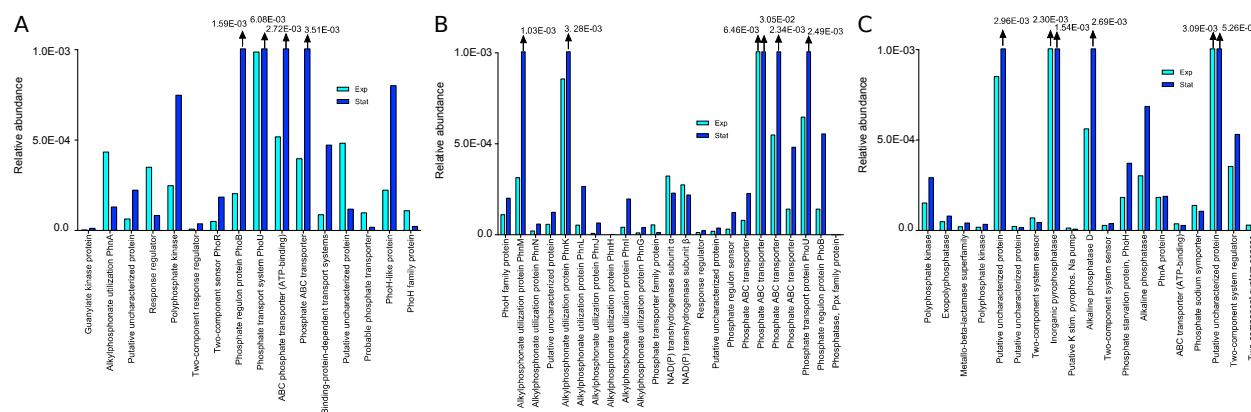
FIG 6. Phosphorus metabolism in all three isolates. List of significantly increasing and decreasing proteins in the SEED category phosphorus metabolism during transition into stationary phase. (A) MED92; (B) MED193; (C) MED134.

SUPPLEMENTARY TABLE LEGENDS

TABLE S1. Individual protein abundances in MED92. Identified proteins with estimated fold change (FC and log2FC columns), false discovery rate (localfdr), readings per sample (exp1-3 for exponential phase; stat1-3 for stationary phase) and various other statistics. Green shades in the log2FC column indicate higher abundance in stationary phase, yellow shades indicate lower; the stronger the color, the larger the difference between growth phases. False discovery rates less than 5% are indicated with green color, above with red.

TABLE S2. Individual protein abundances in MED193. Identified proteins with estimated fold change (FC and log2FC columns), false discovery rate (localfdr), readings per sample (exp1-3 for exponential phase; stat1-3 for stationary phase) and various other statistics. Green shades in the log2FC column indicate higher abundance in stationary phase, yellow shades indicate lower; the stronger the color, the larger the difference between growth phases. False discovery rates less than 5% are indicated with green color, above with red.

TABLE S3. Individual protein abundances in MED134. Identified proteins with estimated fold change (FC and log2FC columns), false discovery rate (localfdr), readings per sample (exp1-3 for exponential phase; stat1-3 for stationary phase) and various other statistics. Green shades in the log2FC column indicate higher abundance in stationary phase, yellow shades indicate lower; the stronger the color, the larger the difference between growth phases. False discovery rates less than 5% are indicated with green color, above with red.

TABLE S4. Top SEED category summaries. Approximate (order of magnitude precision) relative abundances of proteins summed over top categories of the SEED classification. Proteins classified in more than one category were counted in all categories. The calculation of relative

54

abundances counted each protein only once. Log2 fold changes (log2fc) calculated as the ratio between means in stationary phase divided by means in exponential phase. Counts and abundances of the three protein groups, increasing ("Up"), stable and decreasing ("Down") in the three isolates.

TABLE S5. Relative protein abundances summed over second level SEED categories. Approximate (order of magnitude precision) relative abundances of proteins summed over second level categories of the SEED classification. Proteins classified in more than one category were counted in all categories. The calculation of relative abundances counted each protein only once. Log2 fold changes (log2fc) calculated as the ratio between means in stationary phase divided by means in exponential phase.

TABLE S6. Relative protein abundances summed over third level SEED categories. Approximate (order of magnitude precision) relative abundances of proteins summed over third level categories of the SEED classification. Proteins classified in more than one category were counted in all categories. The calculation of relative abundances counted each protein only once. Log2 fold changes (log2fc) calculated as the ratio between means in stationary phase divided by means in exponential phase.

TABLE S7. Summary of transporter families. Number of detected and differentially abundant protein in the three strains per TCDB transporter family.

TABLE S8. Proteins detected in MED92 with their TCDB classifications. The trsphierarchy field describes each protein's place in the TCDB hierarchy. See the TCDB website for explanations (http://www.tcdb.org/superfamily.php). All the other fields, except trspfamily, were taken from the corresponding MED92 SAM table (S1).

56

TABLE S9. Proteins detected in MED193 with their TCDB classifications. The trsphierarchy field describes each protein's place in the TCDB hierarchy. See the TCDB website for explanations (http://www.tcdb.org/superfamily.php). All the other fields, except trspfamily, were taken from the corresponding MED193 SAM table (S2).

TABLE S10. Proteins detected in MED134 with their TCDB classifications. The trsphierarchy field describes each protein's place in the TCDB hierarchy. See the TCDB website for explanations (http://www.tcdb.org/superfamily.php). All the other fields, except trspfamily, were taken from the corresponding MED134 SAM table (S3).